


Three-dimensional imaging of intact porcine cochlea using tissue clearing and custom-built light-sheet microscopy: supplement

ADELE MOATTI,^{1,2} YUHENG CAI,^{1,2} CHEN LI,^{1,2} TYLER SATTLER,^{1,2}
LAURA EDWARDS,^{2,3} JORGE PIEDRAHITA,^{2,3} FRANCES S.
LIGLER,^{1,2} AND ALON GREENBAUM^{1,2,4,*} 

¹Joint Department of Biomedical Engineering, North Carolina State University and University of North Carolina at Chapel Hill, Raleigh, NC 27695, USA

²Comparative Medicine Institute, North Carolina State University, Raleigh, NC 27695, USA

³Department of Molecular Biomedical Sciences, North Carolina State University, Raleigh, NC 27695, USA

⁴Bioinformatics Research Center, North Carolina State University, Raleigh, NC 27695, USA

*greenbaum@ncsu.edu

This supplement published with The Optical Society on 8 October 2020 by The Authors under the terms of the [Creative Commons Attribution 4.0 License](https://creativecommons.org/licenses/by/4.0/) in the format provided by the authors and unedited. Further distribution of this work must maintain attribution to the author(s) and the published article's title, journal citation, and DOI.

Supplement DOI: <https://doi.org/10.6084/m9.figshare.13030583>

Parent Article DOI: <https://doi.org/10.1364/BOE.402991>

Three-dimensional imaging of intact porcine cochlea using tissue clearing and custom-built light-sheet microscopy

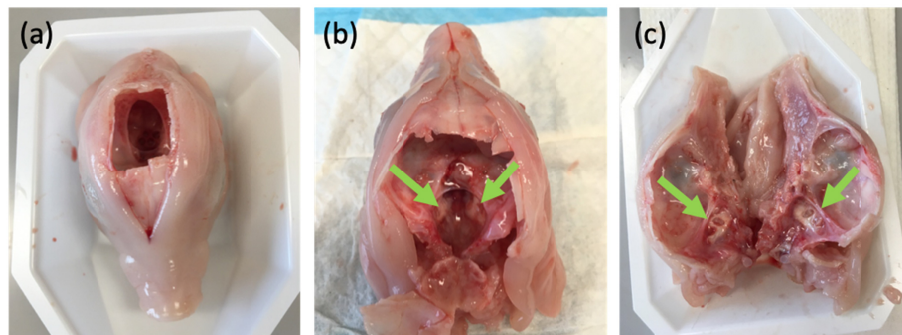


Fig. S1. An 80-days old pig fetus being prepared for cochlea extraction. (a) Carving a window in the skull using a bone-saw and emptying the skull. (b) Creating a wider window to see both cochleae. (c) Cutting the skull in half and carefully cutting the area around the cochlea to prepare it for the decalcification step.

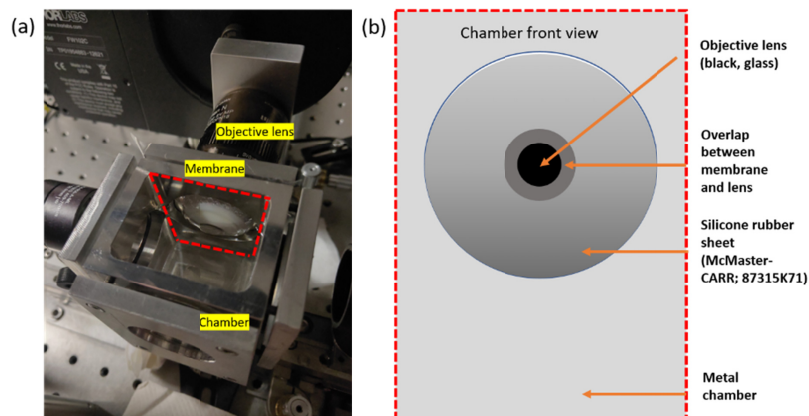


Fig. S2. A silicone membrane is used to minimize potential damage to the objective lens when immersed in DBE. (a) An image of the specimen chamber with the objective lens, which is covered by a silicone rubber sheet and only its glass is in contact with DBE. (b) The drawing shows the high-purity silicone rubber sheet, which covers all the plastic part of the objective lens, and a small portion of the objective lens's glass. This configuration protects the objective from possible chemical damage.

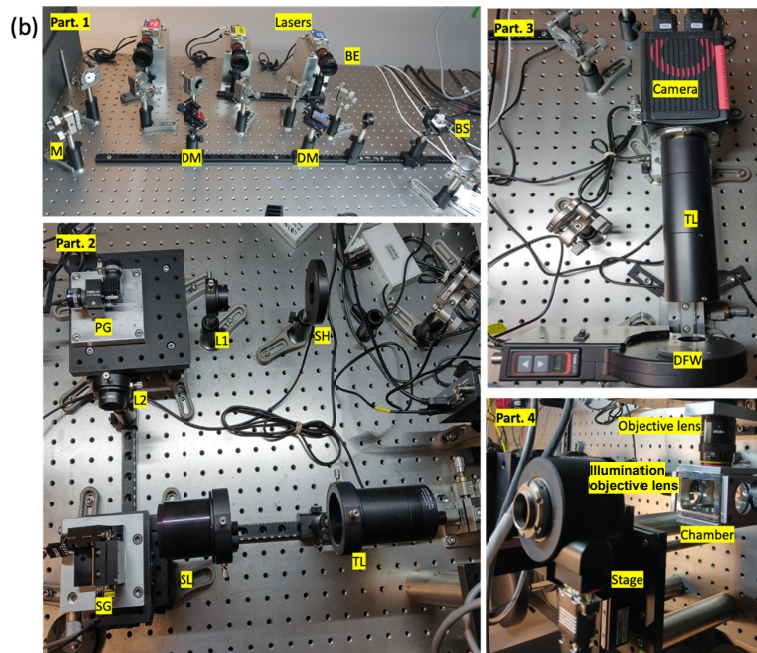
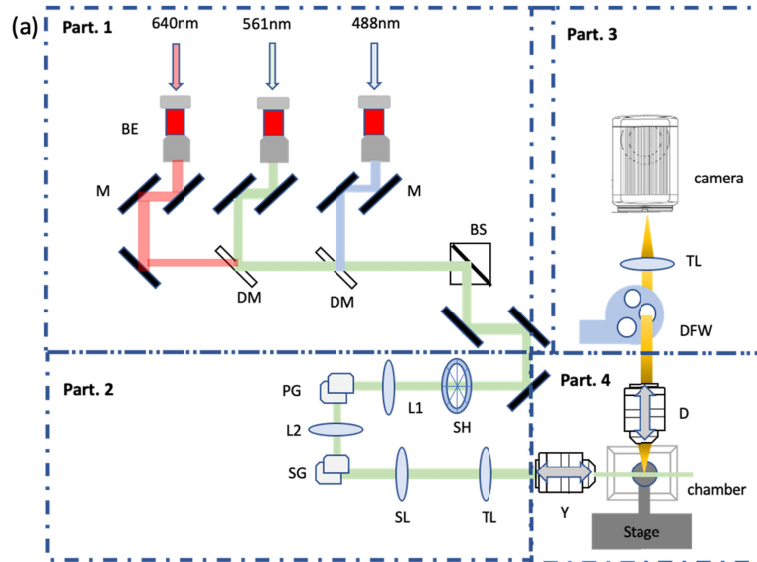


Fig. S3. (a) A schematic diagram of the light-sheet microscope. Part. 1: BE: beam expander; M: mirror; DM: dichroic mirror; BS: beam splitter; Part. 2: SH: shutter; L1(L2): relay lens; PG: pivot galvo mirrors; SG: scan galvo mirror; SL: scan lens; TL: tube lens; Part. 3: DFW: detection filter wheel; Part. 4: D: detection objective lens and motorized actuator; Y: illumination objective lens and motorized actuator. (b) The corresponding pictures refer to the schematic in (a). Part. 1: The illumination system: 488 nm, 561 nm and 640 nm lasers are aligned to share the same light path. Part.2: SG (scan galvo system) and PG (pivot galvo system) are used to generate the light sheet and control its angular properties. Part. 3: Detection system. DFW (detection filter wheel) is used to select different emission wavelength. Part. 4: Imaging chamber, stage, illumination objective lens, and objective lens.

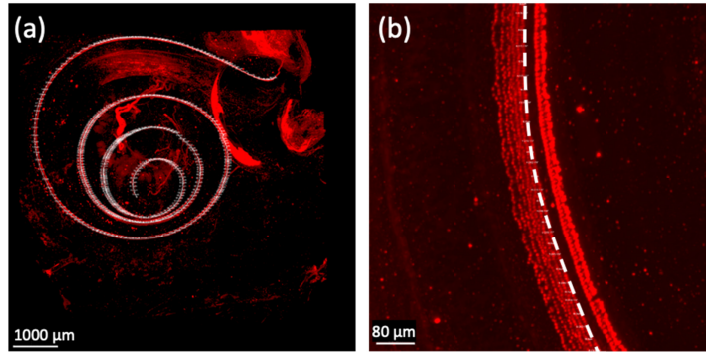


Fig. S4. Spiral tracing procedure. (a) A MIP image that shows the spiral tracing that was performed from apex to basal turn using IMARIS software. (b) A zoom in region, that demonstrates the assignment of the tracing points either at the center of the cochlear duct or in the inner portion of the OHC first row.

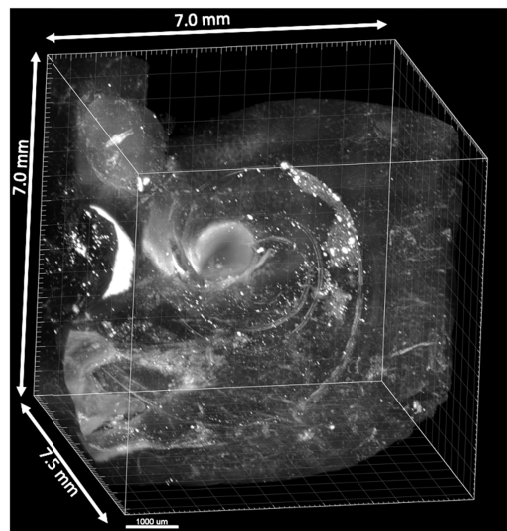


Fig. S5. A 3D reconstruction of an 8-10 w pig's cochlea captured by the custom-built light-sheet microscope. The sample was stained against MYOSIN VIIa. The sample roughly occupies a volume of 250 mm^3 out of the $\sim 367 \text{ mm}^3$ that were imaged.

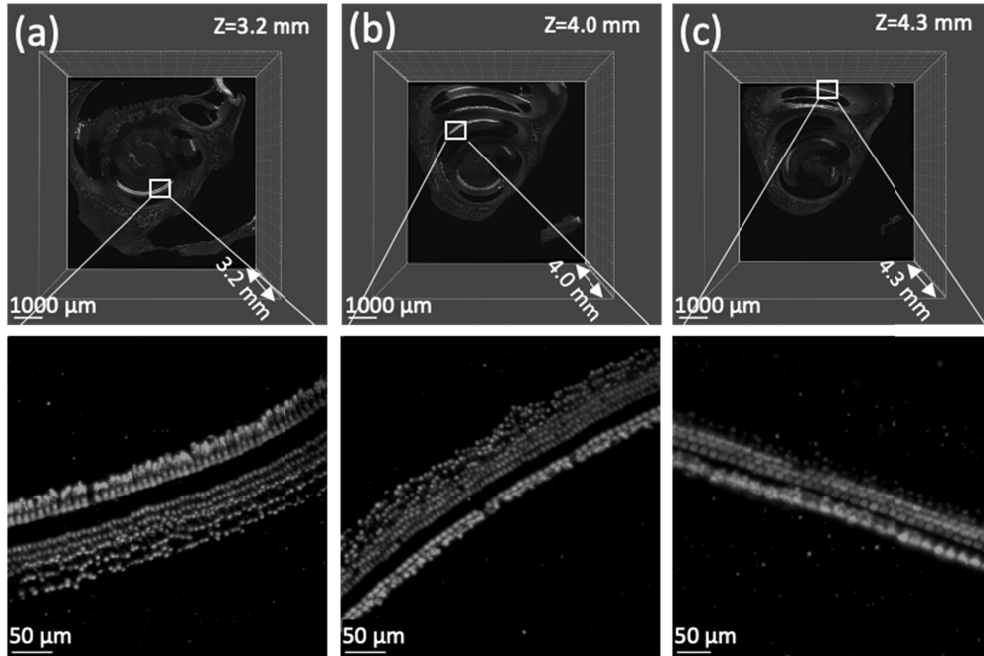


Fig. S6. (a, b, and c) Digital slices (XY plane, 200 μm thick) taken by the custom-built light-sheet microscope at 3.2 mm, 4 mm, and 4.3 mm deep inside a NB pig's cochlea, respectively.

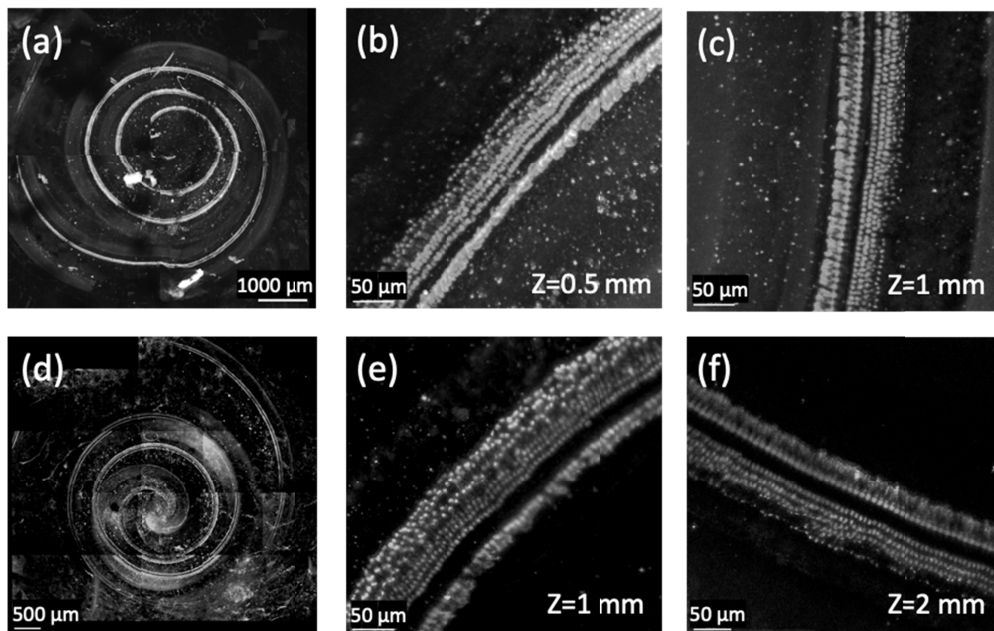


Fig. S7. (a) An 8-10 w pig's cochlea MIP image acquired by a confocal microscope. (b and c) XY plane images at 0.5 and 1 mm deep inside the cochlea (4 \times objective lens, 0.16 NA). (d) A NB pig's cochlea MIP image acquired by a confocal microscope, (10 \times objective lens, 0.75 NA). (e and f) XY plane images at 1 and 2 mm deep inside the cochlea.

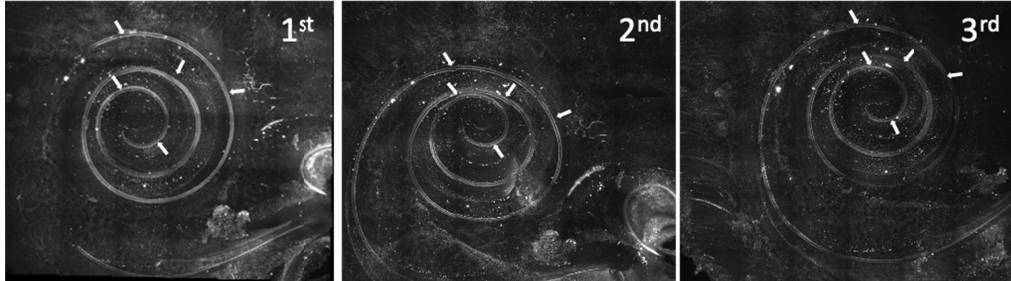


Fig. S8. Areas that were selected for a bleaching analysis are marked by arrows on the MIP of an 8-10 w pig's cochlea after 1st, 2nd, and 3rd time imaging using the custom-built light-sheet microscope.

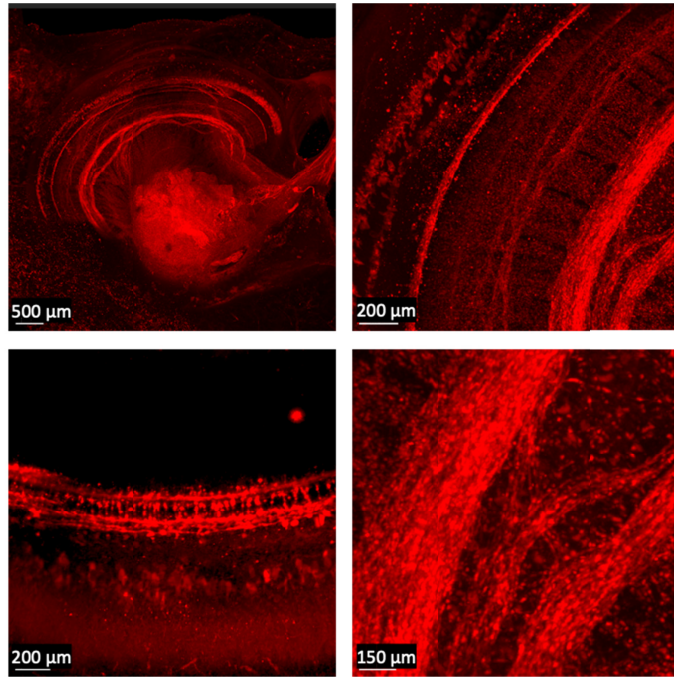


Fig. S9. Micrographs of a NB pig cochlea stained against PGP9.5 that illustrate neuronal innervations at different resolutions. These images were acquired using a confocal microscope (4× objective, 0.16 NA).

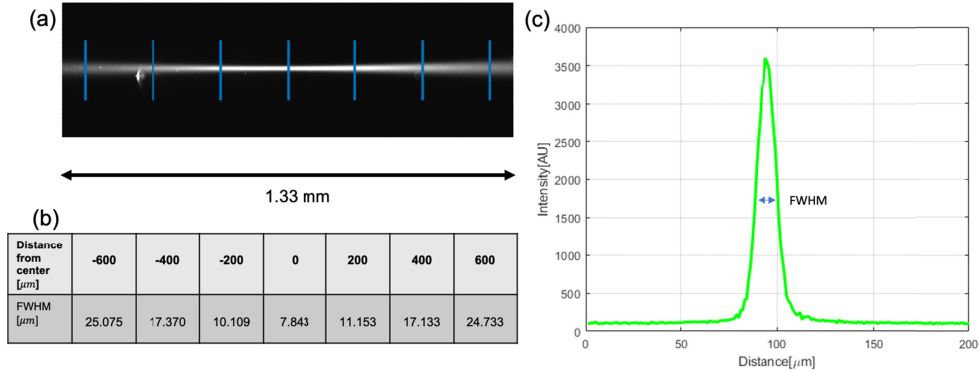


Fig S10. The intensity profile of the illumination beam. (a) An image of the light sheet illumination profile without a sample, when the imaging chamber is filled with DBE. (b) The illumination beam diameter along the field of view. The approximate locations of the cross sections are marked with blue vertical lines in (a). (c) Intensity line profile in the center of the field of view, the full width half maxima (FWHM) is equal to $\sim 8 \mu\text{m}$.

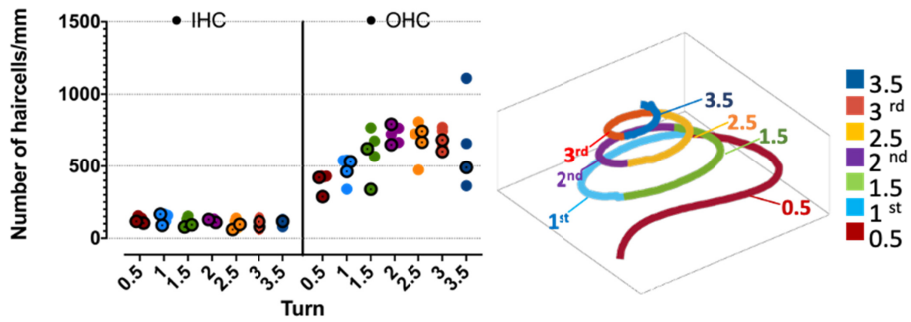


Fig. S11. The IHC and OHC densities (number of hair cells/mm) are presented for each half turn and color-coded to be identified by the inset figure. The newborn pig's data is illustrated by a circle ($n = 3$) and the 8-10 w pig's data is depicted with an outlined circle and a middle dot ($n = 2$). Inset: the schematic diagram of 3D cochlea segmented into half turns and color-coded for each half turn.

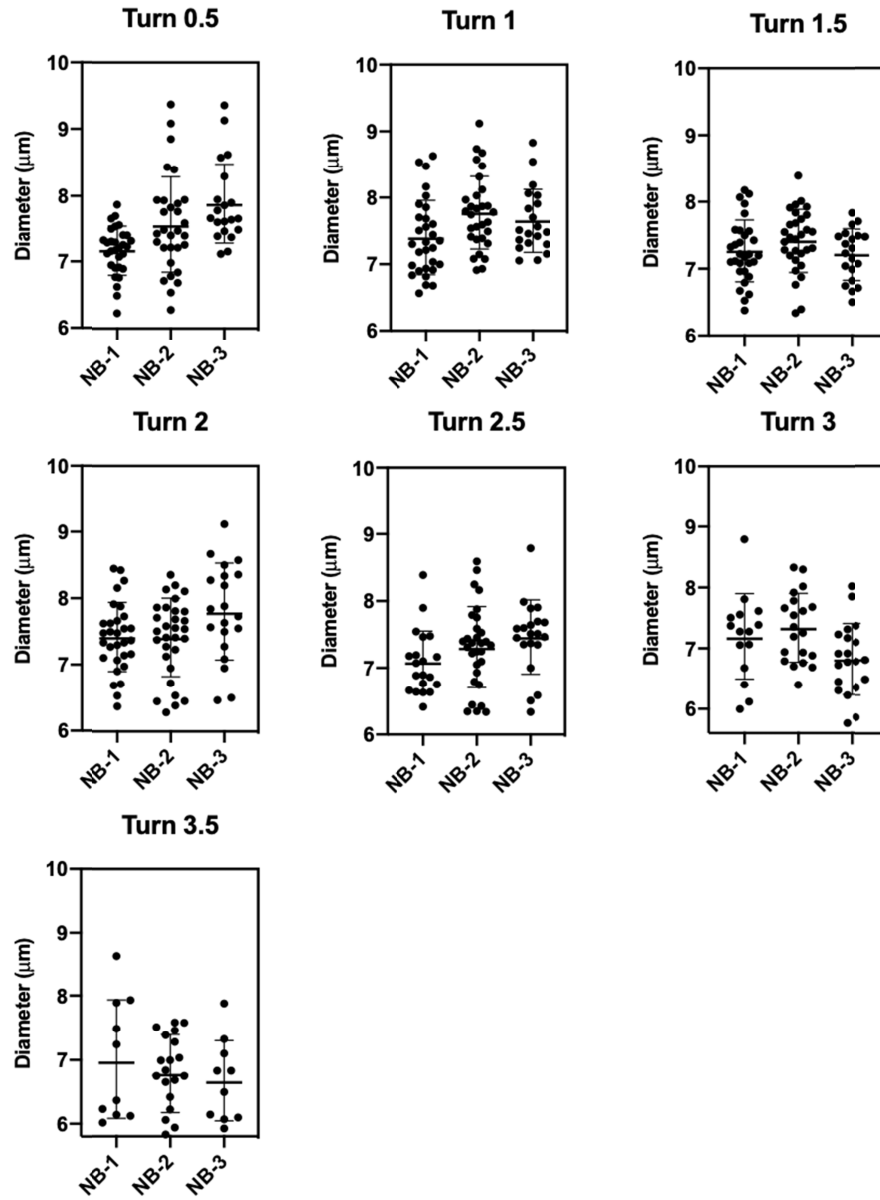


Fig. S12. A comparison between IHC diameter (not length) in different half-turns ($n = 3$; NB pigs) from basal turn (0.5) to apex (3.5). All values are mean \pm SD. Each point represents a cell that its diameter was manually measured.

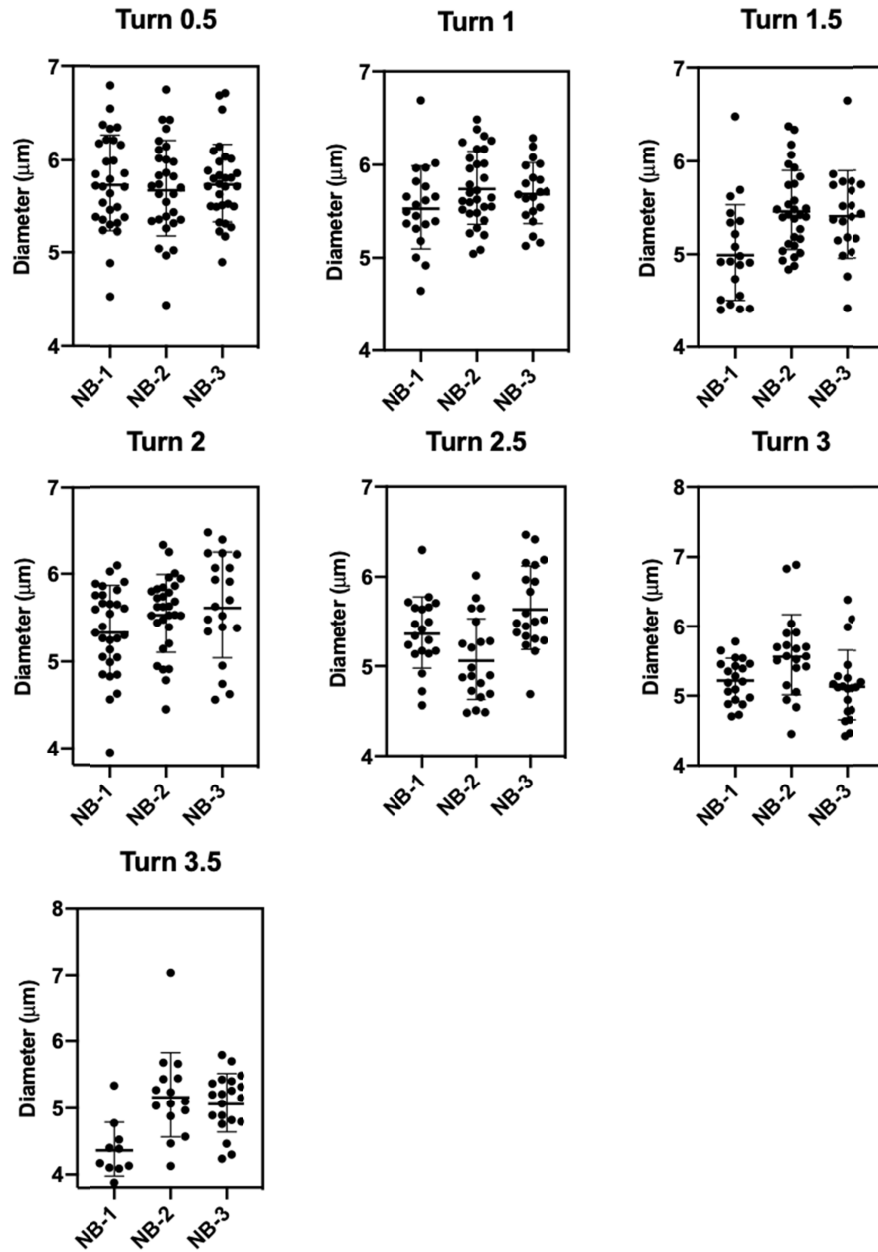


Fig. S13. A comparison between OHC diameter (not length) in different half-turns ($n = 3$; NB pigs) from basal turn (0.5) to apex (3.5). All values are mean \pm SD. Each point represents a cell that its diameter was manually measured.

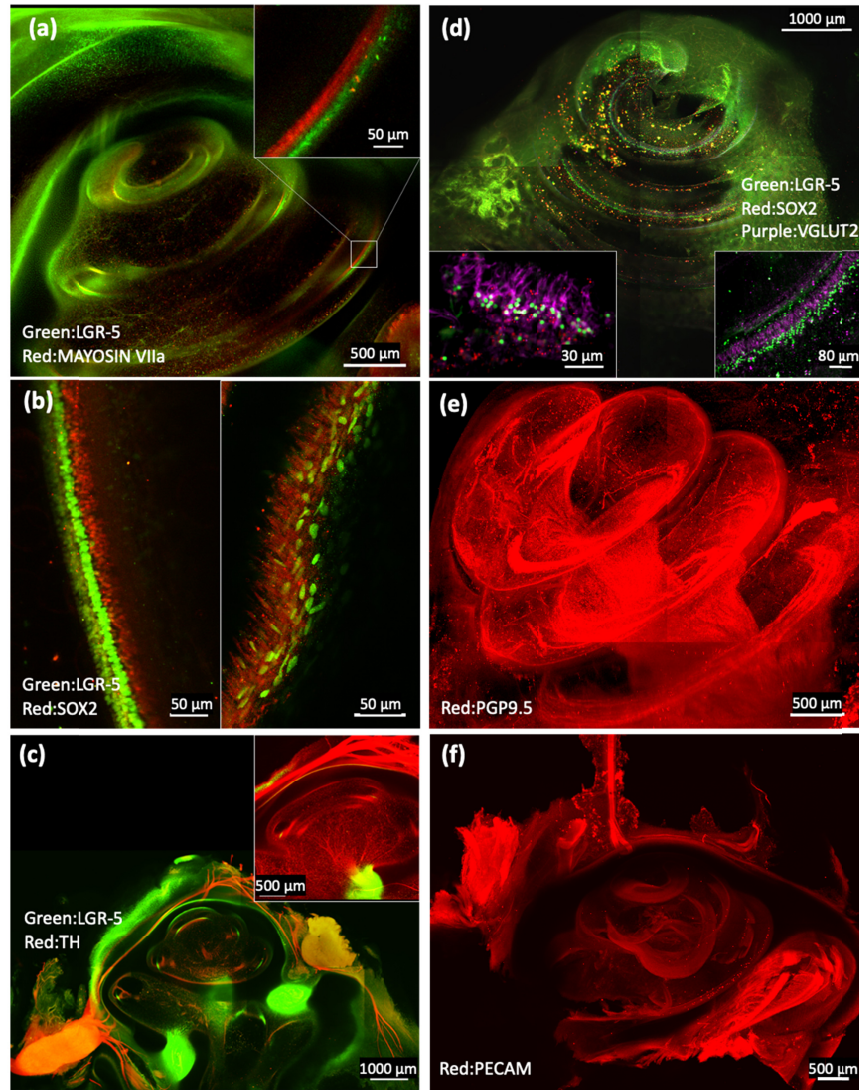


Fig. S14. Applicability to transgenic pig model (50 days old fetus, LGR5-H2B-GFP) and various antibodies. All images were acquired with a confocal microscope. (a) Antibodies against MAYOSIN VIIa and GFP were used to detect hair cells (Red) and LGR5⁺ cells (Green). The zoomed-in region at the inset illustrates the spatial location of the hair cells relative to the LGR5 cells (4× objective lens, 0.16 NA). (b) Digital slices (XY plane) of a cochlea turn stained for anti-GFP (Green) and anti-SOX2 (Red). 30× objective lens, 1.05 NA. (c) Antibodies against TH⁺ (Red) and GFP⁺ (Green) cells were used. The right inset shows sympathetic neuronal innervations surrounding the cochlea (4× objective lens, 0.16 NA). (d) A MIP image of a 50 days old fetus cochlea stained with anti-GFP (Green), anti-SOX2 (Red), and anti-VGLUTII (Purple). 4× objective lens, 0.16 NA. The zoomed-in regions at the inset figures show the stained cells with higher magnification. (e). A MIP image of a newborn pig cochlea (wild type) stained against PGP9.5 (Red). 4× objective lens, 0.16 NA. (f) Antibody against PECAM was used in a 30-days old fetus pig cochlea to detect vasculature (4× objective lens, 0.16 NA).

Table S1. List of primary and secondary antibodies used in the present study

Primary antibody	Company and catalog number
Rabbit Anti-PGP9.5	Proteintech Group, Cat# 14730-1-AP
Rabbit Anti-Tyrosine Hydroxylase	Millipore, Cat# AB152
Chicken Anti-GFP	Aves Labs, Cat# GFP-1020
Mouse Anti-VGLUT2	Abcam, Cat# ab79157
Rat Anti-PECAM1	BD Bioscience, Cat# 553370
Rabbit Anti-MYOSIN VIIa	Proteus, Cat# 25-6790
Rabbit Anti-SOX2	Abcam, Cat# ab97959
Secondary antibody	Company and catalog number
CY3 AffiniPure Donkey Anti-Rabbit IgG	Jackson ImmunoResearch, Cat# 711-165-152
CY3 AffiniPure Donkey Anti-Rat IgG	Jackson ImmunoResearch, Cat# 712-165-153
AF 647 AffiniPure Donkey Anti-Chicken IgY	Jackson ImmunoResearch, Cat# 703-605-155
AF 488 AffiniPure Goat Anti-Chicken IgY	Jackson ImmunoResearch, Cat# 103-545-155
AF 647 AffiniPure Donkey Anti-Mouse IgG	Jackson ImmunoResearch, Cat#715-605-150

Table S2. Light-sheet microscope components.

Component	Part number and description	Manufacturer
Optical table and breadboard	T48W - Nexus Optical Table, 4' x 8' x 12.2", Sealed 1/4"-20 Mounting Holes	Thorlabs
Lasers	OBIS 488-50C, OBIS LS 561-50, OBIS 640-50	Coherent
Beam expander (BE)	GBE03-A, 3X Achromatic Galilean Beam Expander, AR Coated: 400 - 650 nm	Thorlabs
Kinematic mount	KM100S, Kinematic Mount for 1" (25.4 mm) Tall Rectangular Optics, Right-Handed	Thorlabs
Heatsink	12.5cm x 7.5cm x 10.2cm	Custom design
Beam splitter (BS)	BS016,50:50 Non-Polarizing Beamsplitter Cube, 400 - 700 nm, 20 mm	Thorlabs
Dichroic mirrors	25mm x 36 mm Longpass Dichroic Mirror, 505 nm Cut-On; 25 mm x 36 mm Longpass Dichroic Mirror, 605 nm Cut-On	Thorlabs
Tube lens (TL) and illumination objective lens	AC508-180-A-ML, $f=180$ mm, $\varnothing 2$ " Achromatic Doublet, SM2-Threaded Mount, ARC: 400-700 nm AC254-050-A-Mf=50 mm, $\varnothing 1$ " Achromatic Doublet, SM1-Threaded Mount, ARC: 400-700 nm	Thorlabs
Scan lens	CLS-SL, Scan Lens with Large Field of View, 400 to 750 nm, EFL=70 mm	Thorlabs
Shutter	SHB1T, SHM1, Post Mounting Adapter for SHB1(T) Optical Beam Shutter, 8-32 Tap	Thorlabs
Pivot galvo system (PG)	GVS202 - 2D Galvo System, Broadband Mirrors for 400-750 nm; Galvo Driver Card Cover, GCE001; Galvo Mount/Post Adapter Heatsink, Imperial, GHS003	Thorlabs
Scan galvo system (SG)	6215H 5mm Mirrors XY Galvanometer Scanner, Protected Silver	Edmund
4D stage with joystick	Stage-4D-50, three ASI linear stages and a motorized rotating stage that can be controlled by joystick	ASI
Specimen chamber	40mm*30mm*65mm	Custom design
Detection objective lens	XLPLN10XSVMP-2, XLPlan N 10X/0.60 SV MP $\infty/0$ -0.23/OFN18	Olympus
Tube lens	TL180-MMC	ASI
Detection filter wheel (DFW)	6-Position Filter Wheel for $\varnothing 1$ " GFP Emission Filter CWL = 525 nm, BW = 39 nm	Thorlabs
Camera	C13440-20CU	Hamamatsu
Control software	MATLAB2019a	MathWorks
Microscope workstation	CPU: Intel(R) Xeon(R) W-2102 GPU: NVIDIA Quadro P1000, RAM: 32G	Lenovo
Arbitrary Function Generator	AFG31022A	Tektronix
Lens 1 and Lens 2 (L1 and L2)	AC254-125-A-ML, $f=125$ mm, $\varnothing 1$ " Achromatic Doublet, SM1-Threaded Mount, ARC: 400-700 nm	Thorlabs
Motorized linear translation stage	561D-XYZ, and CONEX-TRB12CC motor	Newport

Table S3. Quantification of photo-bleaching after 1st, 2nd, and 3rd time imaging of an 8-10 w pig's cochlea using the custom-built light-sheet microscope

Bleaching evaluation	Region 1	Region 2	Region 3	Region 4	Region 5	Mean	SD
Intensity 1st [a.u.]	4360.33	5247.05	3634.47	4389.13	3824.79	4291.15	627.86
Intensity 2nd [a.u.]	1228.18	2912.89	3289.35	3953.32	2813.65	2839.48	1005.65
Intensity 3rd [a.u.]	900.75	392.50	1011.13	2110.85	1294.93	1142.03	632.28
Ratio (2nd/1st)	0.28	0.55	0.90	0.90	0.73	0.67	0.26
Ratio (3rd/1st)	0.21	0.07	0.28	0.48	0.34	0.27	0.15
Turn	1	1	2	3	3.5	-	-

Table S4. The lower frequency limit calculated based on the radii ratio of the basal over apex turn

Samples	Radii ratio ρ	Frequency (Hz)
NB-1	7.23	41.12
NB-2	7.24	40.95
NB-3	7.26	40.36
Mean	7.24 ± 0.02	40.81 ± 0.40
8-10 W-1	7.33	38.75
8-10 W-1	7.33	38.75
Mean	7.33	38.75 ± 0.00
Total mean	7.28 ± 0.05	39.99 ± 1.16

Note: NB-3 and 8-10 w-1 datasets are collected by the confocal microscope, while the rest of the datasets are captured by the light-sheet microscope. Reported values are mean ± SD.

Table S5. The comparison of inner ear characteristics between different species

Species	60 dB lower frequency limit (Hz)	Basilar membrane length (mm)	Turns	Basilar membrane apex width (μm)	Radii ratio	Ref
Brown bat (<i>Myotis lucifugus</i>)	10300	-	2.25	-	-	[1]
Cat (<i>Felix catus</i>)	55	25.8	3	420	6.2	[2]
Cow (<i>Bos taurus</i>)	23	38	3.5	-	8.9	[2]
Chinchilla (<i>Chinchilla langer</i>)	50	18.5	3	310	6.4	[1,2]
Dog (<i>Canis familiaris</i>)	64	-	3.25	-	-	[1]
Dolphin (<i>Tursiops truncatus</i>)	150	38.9	2.25	380	4.3	[2]
Domestic pig (<i>Sus scrofa</i>)-literature 4 months old	42	38	3.5	-	-	[3,4]
Domestic pig (<i>Sus scrofa</i>)- 0-2 months old	40	33.5	3.5	664	7.3	This study
Elephant (<i>Elephas maximus</i>)	17	60	2.25	-	8.8	[1,2]
Gerbil (<i>Meriones unguiculatis</i>)	56	12.1	3.25	250	6.8	[2]
Guinea pig (<i>Cavia porcellus</i>)	47	18.5	4	245	7.2	[1,2]
Human (<i>Homo sapiens</i>)	29	33.5	2.75	504	8.2	[1,2,5]
Laboratory mouse (<i>Mus musculus</i>)	390	7	2	160	1.7	[1,2]
Rabbit	96	15.2	2.25	-	-	[2]

Table S6. Detailed information of inner and outer hair cell counting in the cochlea for each half turn in NB and 8-10 w pigs' cochleae samples. Quality control (QC).

Sample	Turn	Turn							Total	
		0.5	1	1.5	2	2.5	3	3.5		
NB-1	IHC No	1236.38	967.79	815.61	536.3	514.82	306.49	181.55	4558.94	
	OHC No	4128.36	3333.91	4099.22	3091.65	2700.64	2018.04	1396.75	20768.57	
	Length (mm)	9.71	6.14	5.35	4.05	3.73	2.71	2.12	33.80	
	Raw Length* (mm)	9.71	6.14	5.35	4.05	3.73	2.71	2.12	33.80	
	IHC No/mm	127.38	157.68	152.44	132.50	138.11	113.29	85.44	134.88	
	OHC No/mm	425.32	543.20	766.17	763.84	724.49	745.95	657.34	614.46	
	QC-IHC	Ground Truth	52	59	50	54	48	49	31	
		ilastik	52.01	58.23	50.48	53.8	47.71	50.59	-	
	QC-OHC	Ground Truth	87	72	75	90	67	79	87	
		ilastik	86.48	71.02	74.76	90.52	67.39	79.23	86.65	
NB-2	IHC No	1217.13	1090.14	703.13	556.23	447.23	354.62	248.34	4616.82	
	OHC No	1901.32	3504.33	3030.56	2805.98	1821.67	1926.32	2131.16	17121.34	
	Length (mm)	8.84	6.50	5.33	4.22	3.85	2.50	1.92	33.16	
	Raw Length (mm)	4.42	6.50	5.33	4.22	3.85	2.50	1.92	28.74	
	IHC No/mm	137.67	167.74	131.86	131.75	116.29	141.80	129.29	139.22	
	OHC No/mm	430.13*	539.23	568.32	664.65	473.67	770.28	1109.55	595.72*	
	QC-IHC	Ground Truth	59	47	49	49	49	39	39	
		ilastik	57.51	46.76	48.72	50.34	47.17	38.9	37.75	
	QC-OHC	Ground Truth	73	63	62	97	92	70	72	
		ilastik	72.94	64.66	62.6	98.62	91.93	69.27	72.23	
NB-3, Confocal microscope	IHC No	585.23	812.39	510.86	613.54	281.39	96	128	3027.41	
	OHC No	1621.36	2305.90	3784.11	3333.54	3170.87	1972.68	580.97	16769.432	
	Length (mm)	7.52	6.79	5.60	4.62	3.92	3.11	1.60	33.16	
	Raw Length (mm)	3.76	6.79	5.60	4.62	3.92	1.56	1.60	27.85	
	IHC No/mm	155.62*	119.73	91.15	132.90	71.71	61.73*	79.92	108.71*	
	OHC No/mm	431.15*	339.85	675.15	722.06	808.10	634.2	362.75	570.33*	
	QC-IHC	Ground Truth	46	47	56	53	46	-	-	
		ilastik	44.89	47.39	57.78	51.87	44.45	-	-	
	QC-OHC	Ground Truth	55	69	71	72	79	69	62	
		ilastik	53.58	68.52	72.89	71	78.56	67.66	59.64	
8-10 w-1, Confocal microscope	IHC No	710.86	577.67	430.10	484.28	229.78	242.94	-	2675.63	
	OHC No	1954	3441.12	3443.86	2875.77	2551.16	1836.5	-	16102.41	
	Length (mm)	8.15	6.47	5.54	4.43	3.82	3.05	1.94	33.41	
	Raw Length (mm)	6.79	6.47	5.54	4.43	3.82	3.05	0	30.11	
	IHC No/mm	104.64*	89.25	77.61	109.32	60.11	79.64	-	88.86*	
	OHC No/mm	287.63*	531.65	621.44	649.19	667.40	602.06	-	534.78*	
	QC-IHC	Ground Truth	46	53	74	51	47	34	-	
		ilastik	45.84	52.87	72.3	50.22	47.8	34.37	-	
	QC-OHC	Ground Truth	62	49	89	92	62	58	-	
		ilastik	60.94	48.36	89.58	89.57	62.77	56.31	-	
8-10w-2	IHC No	587.89	639.25	543.92	475.17	341.91	295.39	175.04	3058.57	

	OHC No	2127.5	1775.46	1973.03	2919.40	2656.74	1756.01	731.34	13939.48
	Length (mm)	7.58	5.76	5.84	3.68	3.57	2.57	1.49	30.50
	Raw Length (mm)	5.05	3.84	5.84	3.68	3.57	2.57	1.49	26.05
	IHC No/mm	116.35*	166.4*	93.20	128.95	95.68	114.72	117.33	117.40*
	OHC No/mm	421.06*	462.3*	338.09	792.27	743.49	682.00	490.24	535.04*
QC-IHC	Ground Truth	47	69	45	64	39	41	32	
	ilastik	48.67	70.66	45.84	62.23	40.25	41.14	32.02	
QC-OHC	Ground Truth	60	57	62	78	61	58	48	
	ilastik	59.53	56.67	62.28	77.54	59.27	58.61	47.28	

*Raw length is the length that is considered for hair cells density calculation. The Raw length is different from the actual length due to signal loss or small portions that are not imaged; the density values that are calculated by the Raw length are also marked by *.

Table S7. Inner and outer hair cell diameter in the cochlea for each half turn in NB and 8-10 w pig samples.

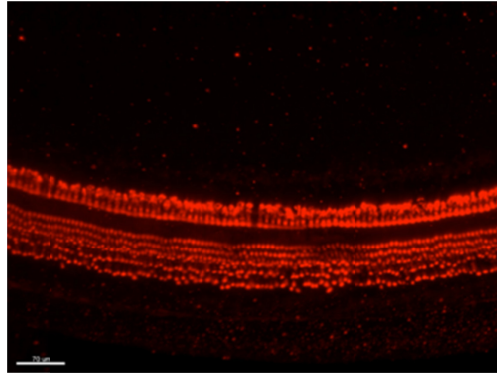
Half-turn	IHC diameter (μm)													
	0.5		1		1.5		2		2.5		3		3.5	
	STD	MEAN	STD	MEAN	STD	MEAN	STD	MEAN	STD	MEAN	STD	MEAN	STD	MEAN
NB-1	7.17	0.36	7.40	0.56	7.26	0.46	7.42	0.52	7.08	0.48	7.19	0.70	7.00	0.95
NB-2	7.56	0.73	7.77	0.55	7.41	0.46	7.41	0.57	7.31	0.60	7.33	0.56	6.78	0.60
NB-3	7.87	0.61	7.65	0.48	7.21	0.38	7.80	0.71	7.46	0.55	6.82	0.58	6.66	0.64

Half-turn	OHC diameter (μm)													
	0.5		1		1.5		2		2.5		3		3.5	
	STD	MEAN	STD	MEAN	STD	MEAN	STD	MEAN	STD	MEAN	STD	MEAN	STD	MEAN
NB-1	5.75	0.50	5.54	0.44	5.01	0.53	5.35	0.49	5.37	0.39	5.22	0.31	4.37	0.42
NB-2	5.69	0.50	5.75	0.39	5.47	0.43	5.54	0.43	5.07	0.45	5.59	0.58	5.19	0.66
NB-3	5.75	0.42	5.69	0.32	5.42	0.47	5.64	0.59	5.65	0.46	5.15	0.51	5.06	0.43

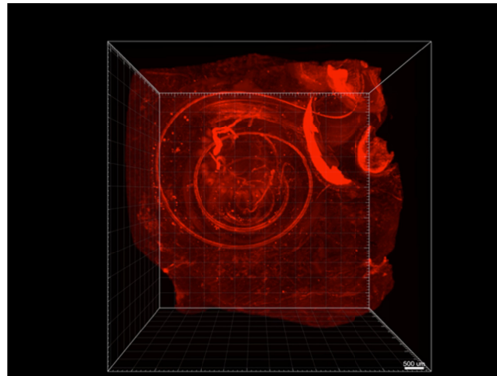
Note: NB-3 dataset was collected by the confocal microscope while the rest of the datasets were captured by the light-sheet microscope.



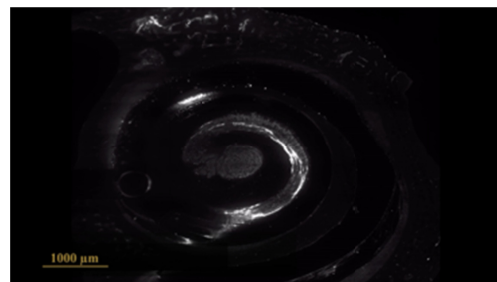
Visualization S1. Extraction of the cochlea after decalcification.



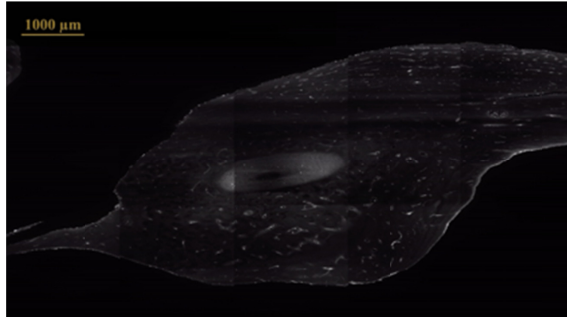
Visualization S2. A 3D reconstruction of an intact cochlea of a pig (8-10 w old) stained against MYOSIN VIIa and imaged with the LSFM.



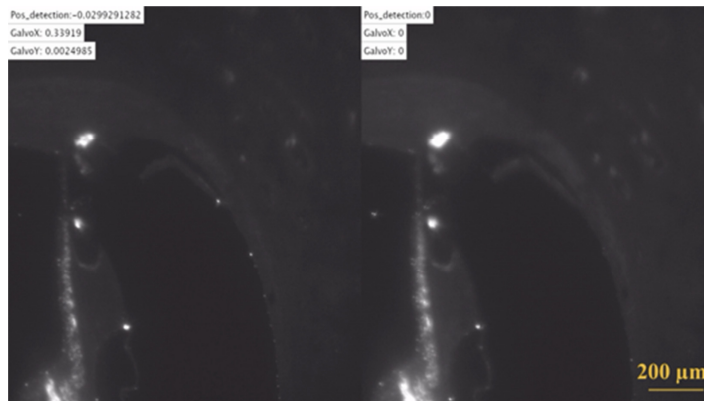
Visualization S3. A 3D reconstruction of a NB pig's cochlea, these images were acquired using the LSFM.



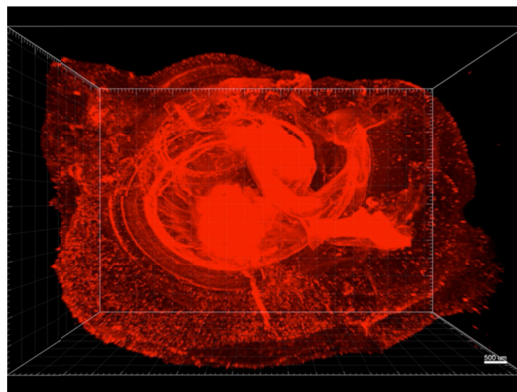
Visualization S4. A trapped air bubble inside an 8-10 w pig cochlear duct. These images were acquired using the LSFM.



Visualization S5. Digital slicing of an 8-10 w old pig stained against MYOSIN VIIa illustrating IHC and OHC rows as well as the whole structure of the cochlear duct, imaged with the LSM.



Visualization S6. A side-by-side comparison of imaging with (left image) and without (right image) adaptive corrections throughout the image stack. The sample is an 8-10 w old porcine cochlea stained against PGP9.5. Galvo X and Y change the pitch and yaw angles respectively.



Visualization S7. Three-dimensional whole-tissue imaging of a pig cochlea stained against PGP9.5. These images were acquired using a confocal microscope (4× objective lens, 0.16 NA).

References:

1. C. D. West, "The relationship of the spiral turns of the cochlea and the length of the basilar membrane to the range of audible frequencies in ground dwelling mammals," *J. Acoust. Soc. Am.* **77**(3), 1091–1101 (1985).
2. D. Manoussaki, R. S. Chadwick, D. R. Ketten, J. Arruda, E. K. Dimitriadis, and J. T. O'Malley, "The influence of cochlear shape on low-frequency hearing," *Proc. Natl. Acad. Sci. U. S. A.* **105**(16), 6162–6166 (2008).
3. R. S. Heffner and H. E. Heffner, "Hearing in domestic pigs (*Sus scrofa*) and goats (*Capra hircus*)," *Hear. Res.* **48**(3), 231–240 (1990).
4. J. M. Lovell and G. M. Harper, "The morphology of the inner ear from the domestic pig (*Sus scrofa*)," *J. Microsc.* **228**(3), 345–357 (2007).
5. D. D. Greenwood, "A cochlear frequency-position function for several species—29 years later," *J. Acoust. Soc. Am.* **87**(6), 2592–2605 (1990).